Graphical Abstract

FBXO22-Deficiency

Unaffected

Affected

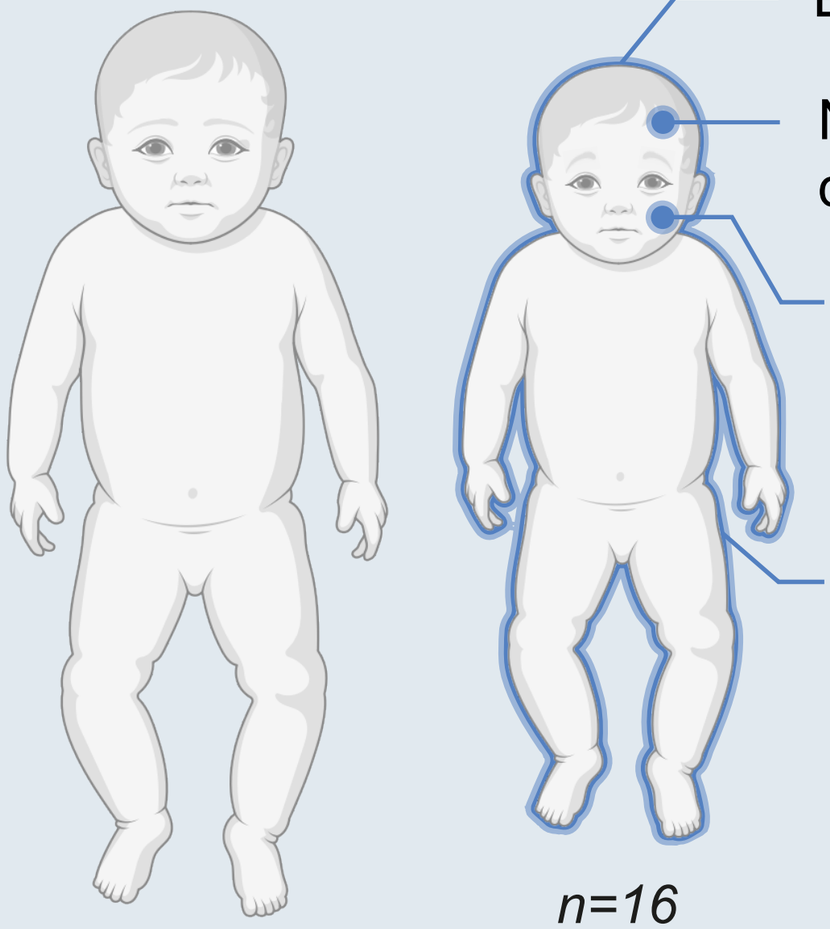

n=16

- Early growth restriction
- Neurodevelopmental delay
- Characteristic craniofacial abnormalities
- Others: cardiovascular, gastrointestinal, urinal & endocrinal abnormalities

FBXO22

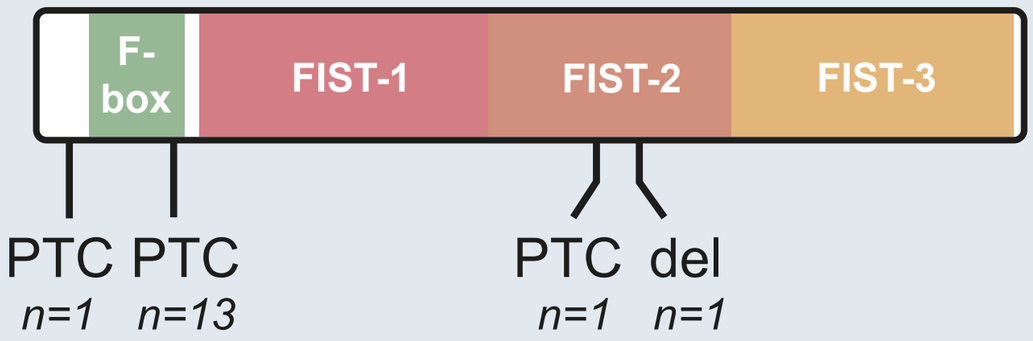

CADD Scores >30
Expected pLoF

Epigenetic Alterations

Affected fibroblasts

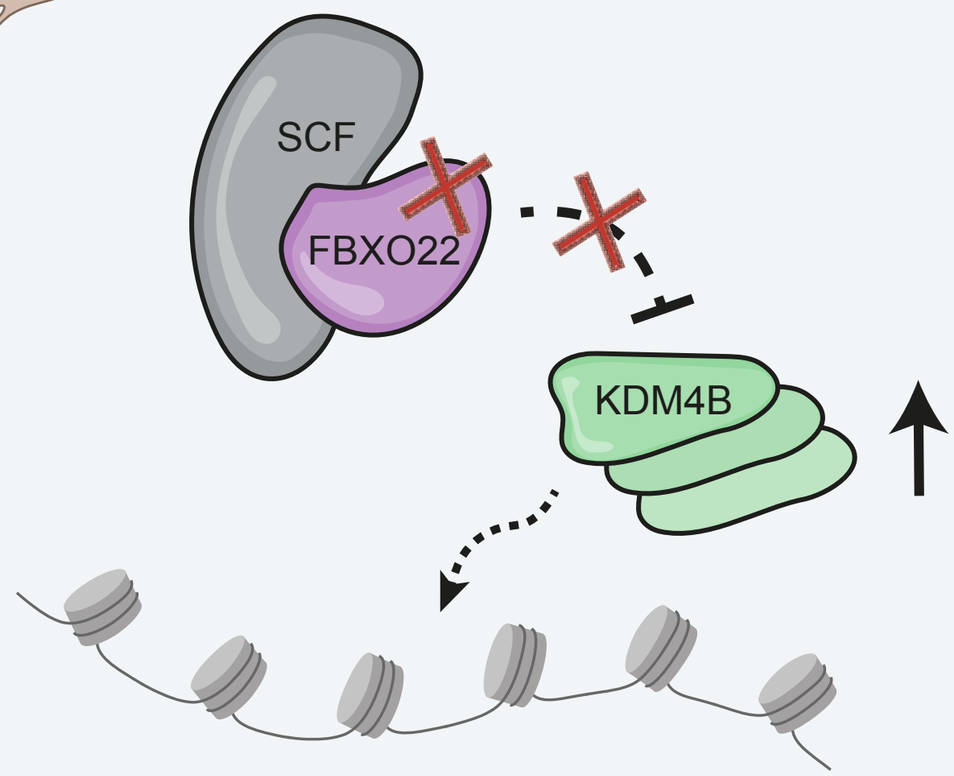

Stabilized KDM4B levels

Peripheral blood

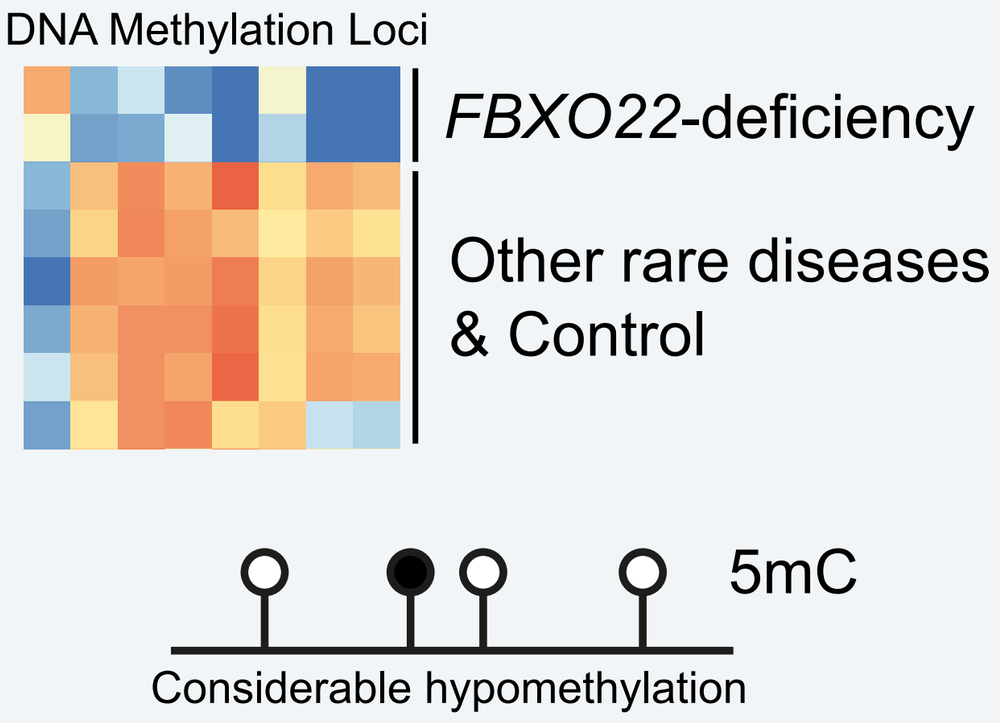

Unique DNA methylation signature

FBXO22 deficiency defines a pleiotropic syndrome of growth restriction and multi-system anomalies associated with a unique epigenetic signature

Navin B. Ramakrishna[1], Umar Bin Mohamad Sahari[1,2,†], Yoshikazu Johmura[3,†], Nur Ain Ali[1], Malak Alghamdi[4], Peter Bauer[5], Suliman Khan[5], Natalia Ordoñez[5], Mariana Ferreira[5], Jorge Pinto Basto[5], Fowzan S. Alkuraya[6], Eissa Ali Faqeih[7], Mari Mori[8,9], Naif A. M. Almontashiri[10,11], Aisha Al Shamsi[12], Gehad ElGhazali[13], Hala Abu Subieh[14], Mode Al Ojaimi[15], Ayman W. El-Hattab[15], Said Ahmed Said Al-Kindi[16], Nadia Alhashmi[17], Fahad Alhabshan[18], Abdulaziz Al Saman[19], Hala Tfayli[20], Mariam Arabi[21], Simone Khalifeh[22], Alan Taylor[23], Majid Alfadhel[24,25], Ruchi Jain[23], Shruti Sinha[23], Shruti Shenbagam[23], Revathy Ramachandran[26,27], Umut Altunoğlu[28], Anju Jacob[29,30], Nandu Thalange[29,30], Mireille El Bejjani[29,30], Arnaud Perrin[1], Jay W. Shin[1,2], Almundher Al-Maawali[31], Azza Al-Shidhani[31], Amna Al-Futaisi[31], Fatma Rabea[26], Ikram Chekroun[26], Mohamed A. Almarri[26,32], Tomohiko Ohta[33], Makoto Nakanishi[34], Alawi Alsheikh-Ali[26,30], Fahad R. Ali[26,27], Aida M. Bertoli-Avella[5,*], Bruno Reversade[1,28,35,36,*,‡], Ahmad Abou Tayoun[23,27,*,‡]

* Joint senior authors.
†These authors contributed equally as co-2nd authors.
‡Correspondence should be addressed to:
Bruno Reversade (bruno@reversade.com)
Ahmad Abou Tayoun (Ahmad.Tayoun@dubaihealth.ae)

Affiliations

1. Genome Institute of Singapore (GIS), Agency for Science, Technology and Research (A*STAR), 60 Biopolis Street, Genome, Singapore 138672, Republic of Singapore
2. Department of Biochemistry, National University of Singapore, Singapore, 119260, Singapore
3. Division of Cancer and Senescence Biology, Cancer Research Institute, Institute for Frontier Science Initiative, Kanazawa University, Kanazawa, Japan
4. Unit of Medical Genetics, Department of Pediatrics, College of Medicine, King Saud University Medical City, King Saud University, Riyadh, Saudi Arabia
5. Centogene AG, Rostock, Germany
6. Department of Translational Genomics, Center for Genomic Medicine, King Faisal Specialist Hospital and Research Center, Riyadh, Saudi Arabia
7. Section of Medical Genetics, King Fahad Medical City, Children's Specialist Hospital, Riyadh, Saudi Arabia
8. Department of Pediatrics, The Ohio State University College of Medicine, Columbus, OH, USA
9. Genetic and Genomic Medicine, Nationwide Children's Hospital, Columbus, OH, USA

10. Center for Genetics and Inherited Diseases, Taibah University, 7534 Abdul Muhsin Ibn Abdul Aziz, Al Ihn, Al-Madinah al-Munawwarah 42318, Saudi Arabia
11. Faculty of Applied Medical Sciences, Taibah University, Janadah Bin Umayyah Road, Tayba, Al-Madinah al-Munawwarah 42353, Saudi Arabia
12. Paediatrics Department, Tawam Hospital, Al-Ain, United Arab Emirates
13. HQ Medical Operations Division, Union71, Abu Dhabi, UAE
14. Maternal Fetal Medicine Department, Kanad Hospital, Al Ain, United Arab Emirates
15. Department of Clinical Sciences, College of Medicine, University of Sharjah, Sharjah, United Arab Emirates
16. Department of Neonatology, Armed Forces Hospital, Muscat, Oman
17. Child Health Department, Royal Hospital, Muscat, Oman
18. Department of Cardiac Sciences, Ministry of National Guard Health Affairs, Riyadh, Saudi Arabia
19. Pediatric Neurology Department, National Neuroscience Institute, King Fahad Medical City, Riyadh, Saudi Arabia
20. Pediatric Endocrinology and Diabetes, American University of Beirut Medical Center (AUBMC), Beirut, Lebanon
21. Department of Pediatrics and Adolescent Medicine, Pediatric Cardiology Division, Children's Heart Center, American University of Beirut Medical Center, Beirut, Lebanon
22. Pediatric Neurology Division, American University of Beirut Medical Center, Beirut, Lebanon
23. Dubai Health Genomic Medicine Center, Dubai Health, Dubai, United Arab Emirates
24. Genetics and Precision Medicine department (GPM), King Abdullah Specialized Children's Hospital (KASCH), King Abdulaziz Medical City, Ministry of National Guard Health Affairs (MNG-HA), Riyadh, Saudi Arabia
25. Medical Genomic Research Department, King Abdullah International Medical Research Center (KAIMRC), King Saud Bin Abdulaziz University for Health Sciences (KSAU-HS), Ministry of National Guard Health Affairs (MNG-HA), Riyadh, Saudi Arabia
26. College of Medicine, Mohammed Bin Rashid University of Medicine and Health Sciences, Dubai Healthcare City, Dubai, United Arab Emirates
27. Center for Genomic Discovery, Mohammed Bin Rashid University of Medicine and Health Sciences, Dubai Health, Dubai, United Arab Emirates
28. Medical Genetics Department, Koç University School of Medicine (KUSOM), 34010, Istanbul, Turkey
29. Al Jalila Children's Specialty Hospital, Dubai, United Arab Emirates
30. Dubai Health, Dubai, United Arab Emirates
31. Child health department, College of Medicine and Health Sciences, Sultan Qaboos University, Muscat, Oman
32. Genome Center, Dubai Police GHQ, Dubai, United Arab Emirates.
33. Department of Translational Oncology, St. Marianna University Graduate School of Medicine, Kawasaki, Japan
34. Division of Cancer Cell Biology, Institute of Medical Science, The University of Tokyo, 4-6-1 Shirokanedai, Minato-ku, Tokyo 108-8639, Japan
35. NUS Cardiovascular-Metabolic Disease Translational Research Programme (CVMD-TRP), Yong Loo Lin School of Medicine, National University of Singapore, 117599, Singapore
36. Laboratory of Human Genetics & Therapeutics, Biological and Environmental Sciences and Engineering Division (BESE), King Abdullah University of Science and Technology (KAUST), Thuwal, Saudi Arabia

ABSTRACT

FBXO22 encodes an F-box protein which acts as a substrate-recognition component of the SKP1-CUL1-F-box (SCF) E3 ubiquitin ligase complex. Despite its known roles in the post-translational ubiquitination and degradation of specific substrates, including histone demethylases, the impact of FBXO22 on human development remains unknown. Here, we characterize a pleiotropic syndrome with prominent prenatal onset growth restriction and notable neurodevelopmental delay across 16 cases from 14 families. Through exome and genome sequencing, we identify four distinct homozygous *FBXO22* variants with loss-of-function effects segregating with the disease: three predicted to lead to premature translation termination due to frameshift effects, and a single amino acid deletion variant which, we show, impacts protein stability in vitro. We confirm that affected primary fibroblasts with a frameshift mutation are bereft of endogenous FBXO22 and show increased levels of the known substrate histone H3K9 demethylase KDM4B. Accordingly, we delineate a unique epigenetic signature for this disease in peripheral blood via long-read sequencing. Altogether, we identify and demonstrate that FBXO22 deficiency leads to a pleiotropic syndrome in humans encompassing growth restriction and neurodevelopmental delay, the pathogenesis of which may be explained by broad chromatin alterations.

MAIN

Ubiquitin-tagged proteasomal degradation of specific proteins is an essential molecular process that contributes to protein turnover, thus regulating many cellular processes, including cell growth, proliferation, and differentiation.[1–3] When the ubiquitin-proteasome system is impaired, the resultant aberrant stabilization of protein substrates can contribute to common diseases such as cancer, and can also lead to developmental defects that result in rare genetic diseases.[4–7] Ubiquitin tagging of protein substrates is performed by several E3 ubiquitin ligases in complex with accessory proteins - one of which includes the SKP1-CUL1-F-box (SCF) RING-finger E3 ubiquitin ligase complex. A family of proteins termed the F-box proteins interact with the SCF via their F-box domains, functioning as the variable substrate-recognition component of the SCF. Three classes of F-box proteins exist classified according to the substrate-recognition domains present: FBXW (WD40 repeat domains), FBXL (leucine-rich repeat) and FBXO (other non-fully characterized domains).[8–10]

FBXO22 is one of 40 FBXO proteins[9,11] annotated in the human genome that is ubiquitously expressed and has been characterized to play a role in the regulation of cancer.[12,13] In particular, FBXO22 has been identified as a regulator of senescence, as well as a promoter of breast and lung cancer during early oncogenesis, while a suppressor of migration and metastasis during late cancer stages, through the interaction with its identified substrates such as KDM4A, KDM4B, TP53, PTEN and KLF4.[12–20] In addition, its interaction with SKP1 of the SCF E3 ligase complex has been experimentally validated.[15,18,20] While a role for FBXO22 in human development has not yet been described, loss-of-function variants of other family members including *FBXO7* (MIM605648), *FBXO11* (MIM607871) and *FBXO31* (MIM609102) have been shown to cause Mendelian diseases - Parkinson Disease 15 (PARK15, autosomal recessive, MIM260300),[21–23] Intellectual Developmental Disorder with Dysmorphic Facies and Behavioral Abnormalities (IDDFBA, autosomal dominant, MIM618089)[24–26] and Intellectual Developmental Disorder, autosomal recessive-45 (MRT45, MIM615979),[27] respectively. Separately, a mouse *Fbxo22* knockout model has been characterized by

gross and severe growth reduction to around half the size of wild-type littermates, alongside low-penetrant postnatal lethality.[14]

Here, we identify a pleiotropic syndrome with prominent early-onset growth restriction and notable neurodevelopmental delay across 16 cases - comprising 15 individuals and one fetus - from 14 families spanning four countries. Through a mixture of exome and short and long-read whole genome sequencing, we identify four distinct homozygous germline *FBXO22* coding variants segregating with the disease following an autosomal recessive mode of inheritance. Three of the alleles are expected to lead to premature translation termination and potentially nonsense-mediated decay arising from frameshift mutations, while the fourth allele is predicted to lead to protein instability. Analysis of primary cutaneous fibroblasts from an affected individual carrying a homozygous frameshift mutation confirmed the absence of FBXO22 which correlated with increased protein levels of one of its known protein substrates KDM4B, while overexpression analysis of the FBXO22 one amino acid in-frame deletion variant resulted in decreased protein stability. Meanwhile, peripheral blood DNA methylation analysis identified a unique epigenetic signature. We propose that these biallelic mutations of *FBXO22* with loss-of-function (LoF) effects lead to an aberrant stabilization of protein substrates as the cause of this previously undescribed pleiotropic syndrome.

In a collaborative international effort of clinicians and scientists, we identified 15 affected children (nine females and six males) and one fetus (16 cases in total) presenting a common core symptomatology of early onset growth restriction, neurodevelopmental delay, craniofacial abnormalities and additional poly-malformations (cardiovascular, gastrointestinal, urinal and endocrinal) (Figure 1A). All individuals belonged to 14 families from four countries of the Greater Middle East region (UAE, KSA, Oman and Lebanon), of which 12 were identified as consanguineous. Of the 16 cases, three passed away (F7-II:1, F9-II:1 and F13-II:4) and one was a second-trimester Termination of Pregnancy (TOP) of unknown sex (Figure 1 and Table S1).

The 15 affected children who were clinically assessed presented with a severe growth retardation phenotype with intrauterine growth restriction (HP:0001511) (73.3%), short stature (HP:0004322) (66.7%), decreased body weight (HP:0004325) (60%), and an overall failure to thrive (HP:0001508) (86.7%) (Table 1 and Table S1). Among individuals for which precise measurements were available, 83.3% (5/6) were falling at or below -2 Standard Deviation (SD) for birth weight, 100% (6/6) had postnatal weights at or below -2 SD, and 100% (6/6) has postnatal heights below -3 SD (Table S1). In addition, an apparent neurodevelopmental phenotype was observed, with the vast majority of individuals suffering from neurodevelopmental delay (HP:0012758) (86.7%), together with microcephaly (HP:0011451) (73.3%), intellectual disability (HP:0001249) (46.7%), muscular hypotonia (HP:0001252) (66.7%), generalized hypotonia (HP:0001290) (53.3%), frequent seizures (HP:0001250) (53.3%) and poor suck (HP:0002033) (40%) (Table 1 and Table S1).

Furthermore, stark yet similar abnormal craniofacial abnormalities (HP:0001999) were observed across the individuals (80%), as demonstrated here in images of seven individuals encompassing three of the four variants, (where available, obtained with parental consent) (Figure 1B). The craniofacial phenotype included a high forehead (HP:0000348) (53.3%), depressed nasal bridge (HP:0005280) (60%) and short nose (HP:0003196) (33.3%), hypertelorism (HP:0000316) (46.7%) with short palpebral fissure (HP:0012745) (33.3%) and low-set ears (HP:0000369) (40%) (Figure 1B, Table 1 and Table S1). The facial phenotype in affected individuals may show temporal evolution, most evident in a three-year-long and a 12-year-long facial photograph time-lapse for individuals F7-II:3 and F2-II:3, respectively (Figure 1B). In infancy, the face tends to be round with sparse eyebrows and bears a superficial resemblance to that observed in type II collagen defects due to a depressed nasal bridge and a short nose. Over time, the face becomes triangular and eyebrows become horizontal with a downward lateral curve, while still demonstrating medial sparsity. This distinctive eyebrow morphology may provide a diagnostic handle for the *FBXO22*-related phenotype in older children.

Although the growth impairment, neurodevelopmental delay and craniofacial anomalies were the most apparent, additional phenotypes with clinical variability were also observed. Cardiovascular defects were noted with atrial septal defect (HP:0001631) (26.7%) and patent ductus arteriosus (HP:0001643) (33.3%), as well as gastrointestinal defects with gastroesophageal reflux (HP:0002020) (33.3%), duodenal atresia (HP:0002247) (40%) and feeding difficulties (HP:0011968) (40%) (Table S1). Several individuals additionally showed skeletal presentations with hip dislocation (HP:0002827) (26.7%), as well as camptodactyly (HP:0100490) (20%) with tapered digits (HP:0001182) (20%), as demonstrated by individuals F2-II:3 and F7-II:1 (Figure 1C and Table S1). The fingers of these two individuals showed a resemblance to that characteristic of Coffin-Lowry syndrome (MIM303600), in exhibiting a soft appearance with distal tapering. Some of the affected individuals also showed variable endocrine abnormalities, including hyperthyroidism (HP:0000836) (6.7%) and hypothyroidism (HP:0000821) (26.7%) (Table S1).

To identify the underlying genetic cause of this pleiotropic syndrome, we performed either exome sequencing, or short and/or long-read genome sequencing on the affected individuals from all 14 families (full details in Table S1). Four distinct germline variants in *FBXO22* (NM_147188.3, MIM609096) with LoF effects were identified across the 14 families, with affected individuals carrying biallelic variants (Figure 1A). Full segregation was observed in families that were tested (9/9). This agreed with the likely Mendelian recessive mode of inheritance across the largely consanguineous backgrounds of the families, with no sex-linked segregation observed. The majority of individuals (families F1-8, F11-13) had the homozygous allele c.159_162del, while F9-II:1 bore the homozygous allele c.8_36del, F10-II:7 harbored the homozygous c.719_722del allele and F14-II:1 bore the homozygous allele c.663_666delinsG. All four variants have not been annotated in public databases (gnomAD v4.1.0 - Figure 1D, ExAC, BRAVO/TOPmed) in either the heterozygous or homozygous states, alluding to their rarity.

FBXO22 spans 7 exons, encoding the 403-amino-acid-long FBXO22 comprising two major domains: an N-terminal SCF-interacting F-box domain, and the protein substrate interacting F-box and Intracellular Signal Transduction (FIST) domain, arranged in three subdomains (FIST-1, FIST-2 and FIST-3) adopting a threefold pseudosymmetry. (Figure 2A).[9,13,14,18,28–30] Three of the variants encode frameshift alleles predicted to result in premature termination codons (PTCs) - c.8_36del; p.(Pro3Leufs*13), c.159_162del; p.(Arg53Serfs*13), and c.719_722del; p.(Val240Alafs*6). The fourth allele results in an effective three bp deletion, resulting in a single amino acid loss in the FIST-2 sub-domain - c.663_666delinsG; p.Val222del. All four variants showed the highest combined annotation-dependent depletion (CADD)[31] scores of within 31 to 35 (Figure 1D), indicating that they are predicted to be highly deleterious.

Disruptive truncating variants are expected to result, with both p.(Pro3Leufs*13) and p.(Arg53Serfs*13) occurring at the N-terminus, and p.(Val240Alafs*6) truncating part of the substrate-recognizing FIST domain, removing half of the FIST-2 sub-domain and the whole FIST-3 sub-domain (Figure 2A). In particular, two of the three frameshift variants (p.(Arg53Serfs*13) and p.(Val240Alafs*6)) are anticipated to additionally lead to nonsense-mediated decay (NMD) due to the presence of PTCs in exon 2 and 6, respectively, of the 7-exon transcript, with the PTC of c.719_722del; p.(Val240Alafs*6) located 77 nucleotides (nt) upstream from the final exon-exon junction, also meeting the criteria for NMD (having a PTC within the upstream exons, and >55 nt away from the final exon-exon junction if within the penultimate exon).[32–34] In addition, while c.8_36del; p.(Pro3Leufs*13) is located in a typically NMD-escape region (with the frameshift occurring within the first 150 nt from the start codon) potentially allowing for translation re-initiation[35,36], no alternative start codons are present upstream, while the second and third AUG downstream are out of frame and occur in NMD-predicted regions yielding 41 or 51 nonsense peptides respectively (Figure S1A). In the event these do not lead to NMD, the fourth AUG would theoretically yield an N-terminal F-box and FIST-1 truncated protein, abrogating its interaction with the SCF E3 ligase complex (Figure S1A).

For the fourth allele - c.663_666delinsG; p.Val222del, a destabilized FBXO22 fold or impaired interaction with its substrates is anticipated. Notably, the affected individual exhibits striking craniofacial and phenotypic similarities to those with the PTC variants, suggesting a common underlying LoF etiology (Figure 1B, Table S1). Valine^{222} is highly conserved in mammals, and occasionally replaced by another hydrophobic residue in vertebrates (Figure S1B). Of note, the residue is not near observed post-translational modifications within FBXO22 (UniProt:Q8NEZ5). In silico analysis of AlphaFold3 and recently-generated cryo-EM structures (which align well, Figure S1C) places Val^{222} within a beta-strand interacting with the interior hydrophobic core of the FIST-2 subdomain (Figure S1C)[29,30,37], suggesting its role in contributing to stabilization of the substrate-interacting FIST domain. AlphaFold3 modelling of the p.Val222del variant (Figure S1D) shows increased Predicted Aligned Error (PAE) in the FIST-2 sub-domain (Figure S1E), alongside a decreased overall mean whole-protein predicted local distance difference test (pLDDT) score, a per-residue measure of local confidence (76.9 vs. 80.68 in WT), altogether indicating lower confidence in the fold. To predict the impact of the single amino acid deletion p.Val222del on protein stability,[38] the free energies of FoldX-repaired structures of WT and p.Val222del were calculated, with the variant having an unfavourable ΔG of folding of +13.954 kcal/mol and a ΔΔG of +17.520 kcal/mol compared to the WT (Figure S1E), further supporting instability, particularly in the FIST-2 domain.

In further support of the pathogenicity of the LoF variants, we note that *FBXO22* is entirely devoid of biallelic occurrences of rare (≤0.5%) LoF (with no biallelic homozygous truncating variants) and/or deleterious (predicted) missense variants in gnomAD (variant co-occurrence statistics only available in v2.1.1). Interestingly, a strong founder mutation likely exists in the Greater Middle East from which all of the affected individuals originate. The c.159_162del; p.(Arg53Serfs*13) variant has a minor allele frequency of 0.05% in Qatar, where 15 heterozygous individuals were ascertained within a healthy cohort of 14,000 whole genomes. In addition, haplotype analysis of the c.159_162del; p.(Arg53Serfs*13) variant across all three long-read whole genome-seq samples (from families F1, F7 and F12; Table S1) show that it lies on a haplotype inferred to be of Middle Eastern ancestry (Figure S2A and B), while phylogeny analysis show that all six

haplotypes (two per individual) cluster together within a larger phylogeny of haplotypes of 135 published Middle Eastern individuals (Figure S2C).[39]

Additionally, the DECIPHER database (GRCh38 v11.28) reports 11 individuals with an additional copy of *FBXO22* due to duplications ranging from 0.4 to 79.4 Mb (whole chromosome duplication) on chromosome 15q24.2. While a phenotype was reported for five individuals, this cannot be disentangled from the duplication of additional genes within the duplicated regions (> 2.31 Mb). Additional searches in public databases have identified that *FBXO22* had no hits in public PheWAS, but some genome-wide significant hits in GWAS for kidney function (NHGRI-EBI GWAS Catalog: GRCh38.p14 and dbSNP Build 156). *FBXO22* was deemed a hit 27 times in 1,356 CRISPR screens (BioGRID ORCS v1.1.16.1), in which its targeted inhibition was often associated with decreased cellular proliferation (52% of hits). This can be interpreted to be in concordance with the gross growth reduction seen across affected individuals and in the mouse KO model.[14]

To assay the pathogenicity of the frameshift variants in the ubiquitously expressed *FBXO22*, with noted elevated levels in brain tissue and cultured fibroblasts (GTEx, Figure S3A), we derived primary cutaneous fibroblasts from individual F7-II:3 bearing homozygous alleles of the most common variant in our cohort (c.159_162del; p.(Arg53Serfs*13)), which was additionally verified by Sanger sequencing. As the variant was predicted to result in a PTC in an early exon, which probably leads to NMD, an RT-qPCR analysis was performed on cDNA extracted from the affected fibroblasts alongside previously derived unaffected wildtype (WT) primary fibroblasts.[40] A significant 2.5-fold reduction in *FBXO22* mRNA levels was noted, down to 40% of the amount seen in the control WT fibroblasts (Figure 2B). In addition, Western blotting analysis demonstrated that endogenous FBXO22 levels were completely absent in the cellular extracts of the affected individual's fibroblasts compared to the WT control (Figure 2C). These results indicate that this frameshift variant likely destabilizes *FBXO22* mRNA via NMD and behaves as a LoF protein-null allele, in agreement with the above predictions. To determine if NMD occurs, we treated WT and affected fibroblasts with the translation inhibitor cycloheximide (CHX), a known NMD inhibitor. A significant 1.7-fold increase in

FBXO22 mRNA levels in affected fibroblasts was observed 24 hours upon CHX treatment, while no change was observed for WT cells between 0 and 24 hours (Figure 2D), implying the contribution of NMD in destabilizing *FBXO22* mRNA variant c.159_162del; p.(Arg53Serfs*13) levels.

As FBXO22 is a characterized substrate-recognition partner of the E3 ubiquitin-ligase SCF complex with known protein targets subject to ubiquitin-tagged proteasomal degradation, we investigated the impact of the loss of FBXO22 on its protein substrates. In particular, we investigated a key known substrate that interacts with FBXO22 at its FIST-3 sub-domain - the ubiquitously expressed epigenetic histone H3K9me3/2 demethylase KDM4B[13,19,41,42] (GTEx, Figure S3B) via RT-qPCR and Western blotting of fibroblast extracts. While the mRNA expression levels of *KDM4B* (MIM609765) in the affected individual's cells were unperturbed compared to the WT control (Figure 2E), a stark increase in KDM4B levels was observed in the affected fibroblast line (Figure 2F). This result highly suggests that KDM4B levels were post-translationally stabilized in the absence of SCF^{FBXO22} proteasomal-degradation activity, with no change to the upstream transcription of its gene.

Separately, to better understand the pathogenicity of the single amino acid deletion p.Val222del variant, we transiently overexpressed FLAG-HA-tagged (*FH-FBXO22*) WT and variant *FBXO22* constructs in HEK293T cells and determined their steady-state protein levels in order to ascertain their stabilities. While both overexpressed *FH-FBXO22* constructs yielded equivalent mRNA levels (Figure 2G), FH-FBXO22-p.Val222del levels were significantly reduced to 60% of WT levels (Figure 2H,H′). This is in agreement with the aforementioned predicted protein instability of the p.Val222del variant as a contributing factor to the pathogenicity of the allele.

Given the observed altered protein levels of the histone demethylase KDM4B in affected fibroblasts, which suggest changes to chromatin in the absence of FBXO22, we turned our attention to profiling epigenetic changes in available affected individuals' samples. Notably, heterozygous LoF variants in *KDM4B*, associated with the autosomal dominant

intellectual development disorder MRD65 (MIM619320), have been previously associated with a robust DNA methylation epigenetic signature in peripheral blood.[43–45] Additional unique DNA methylation epi-signatures have also been identified in Mendelian disorders caused by mutations in other histone demethylases and methyltransferases, with general changes in histone modifications also previously shown to impact DNA methylation.[46–49] We therefore investigated the changes to the DNA methylomes of peripheral blood gDNA from three affected individuals samples from families F1, F7 and F12 with the c.159_162del; p.(Arg53Serfs*13) variant using long read Oxford Nanopore Technology sequencing (ONT-seq) with 5-methylcytosine base calling.

Focusing our DNA methylation analysis across 3,643 genomic loci corresponding to probe regions of previously identified epi-signatures encompassing 34 Mendelian neurodevelopmental disorders (EpiSign MNDD-cohort),[45,50,51] we observed that all three *FBXO22* samples formed a distinct cluster, segregating away from the EpiSign MNDD-cohort and control, implicating a unique *FBXO22*-deficiency epi-signature (Figure S4A). We iteratively identified the top 40 differentially-methylated loci representing a proposed *FBXO22*-specific epi-signature (Supplementary Methods and Table S2).[51] This consists largely of hypomethylation (Figure 3A and Table S3), with *FBXO22*-deficiency samples forming a specific cluster relative to the EpiSign MNDD-cohort and control in principal component analysis of methylation values of these loci (Figure 3B). Analysis of these 40 loci revealed differential methylation in genes or proximal regulatory elements upstream of genes (20 regions out of 40) (Table S3). These genes are found to be predominantly active in the brain (12/20), respiratory system (6/20), gastrointestinal tract (5/20), muscle tissues (8/20 genes), and bone marrow (4/20), and have been associated with neurological and developmental disorders (12/20),[52–56] cardiovascular and blood disorders (6/20)[57,58] and various forms of skeletal abnormalities (4/20)[53,59] (Table 2). A patent finding is significant hypomethylation within the ultimate exon 19 of *AGAP2* (MIM605476) coding for its 3′-UTR in comparison to both the EpiSign MNDD-cohort as well as an additional sample set of unrelated neurological disorders (ND-cohort), previously generated using the same ONT-seq long read sequencing protocol (n=17)[51] (Figure 3C,D). Hypomethylation at the *AGAP2* 3′-UTR has previously been associated

with haploinsufficiency of the H3K4 methyltransferase *KMT2D* in individuals with Kabuki syndrome 1 (MIM147920)[60,61]. Notably, *FBXO22*-deficient individuals and Kabuki cases present with overlapping clinical features such as developmental delay, growth failure, hypotonia and seizures.

Separately, analysis of the methylation profile across regions previously shown to define a specific *KDM4B*-deficiency epi-signature[45] did not show any difference for samples with biallelic *FBXO22* loss-of-function (n=3) in comparison with the ND-cohort (Figure S4B). This result may suggest that although the known *KDM4B* epi-signature is associated with *KDM4B* loss of function, the underlying DNA methylation marker loci might not be dosage-dependent to capture the opposite pattern of resultant KDM4B overexpression associated with *FBXO22* biallelic loss, notwithstanding the confounded effects from likely stabilization of additional FBXO22 targets.

Overall, the ubiquitous expression of *FBXO22* across tissues lends support to the pleiotropic nature of the syndrome, with the demonstrated loss of FBXO22 and accompanying NMD for the tested variant in our fibroblasts from an affected individual leading to an ectopic stabilization of a prototypical protein substrate. Importantly, the interaction between KDM4B and FBXO22 has been documented to occur at the FIST-3 sub-domain, with the involvement of bridging interaction from ESR1/ESR2 at FIST-1 sub-domain in MCF7 breast cancer cells.[19] These estrogen receptors are also noted to be expressed in cultured dermal fibroblasts,[62] in which the stabilization of KDM4B was observed upon FBXO22 loss. Separately, it will be additionally useful in future to determine if NMD similarly occurs for the other two frameshift variants, for which fibroblasts from affected individuals were unavailable. Meanwhile, partial decreased protein levels in line with predicted instability of the p.Val222del variant was apparent. It will also be of interest to determine whether the p.Val222del variant impairs interactions between FBXO22 and its protein targets in relevant cell types.

In addition to KDM4B, additional epigenetic substrates subject to polyubiquitination-targeted protein degradation by SCF^{FBXO22} have been identified to date, which include the

histone demethylases KDM4A and KDM5A.[16,18] Further characterized substrates include the tumor suppressors and cell cycle regulators KDM4A-methylated TP53 (p53), HDM2, PTEN, CDKN1A (p21), CDKN1C (p57Kip2), LKB1, as well as additional targets KLF4, BACH1, BACH2, CD274 (PD-L1), CD147, RPL6 and FKBP12.[14,15,17,20,63–72] Beyond ubiquitin-mediated protein degradation, MTOR (mTOR) has additionally been identified as a non-proteolytic monoubiquitinated substrate of FBXO22, serving a regulatory role in amino acid level sensing.[73,74] With the vast majority of studies performed in cancer cell lines, the repertoire of substrates largely discovered has thus implicated FBXO22 as an epigenetic multiplayer in carcinogenesis and therapy response, particularly as a regulator of senescence, as well as a promoter of breast and lung cancer proliferation in early cancer stages, while a suppressor of migration and metastasis during late cancer stages.[12,13,16,63] To date, no predisposition to or protection against cancer has been documented in the probands, nor in the aforementioned mouse KO line, which instead demonstrated severe growth reduction and occasional early postnatal lethality.[14] In future, it will be informative to understand how the remaining substrates of FBXO22 are impacted across various tissues in *FBXO22*-deficiency.

The observed stabilization and increase in KDM4B levels in affected fibroblasts, together with knowledge of additional epigenetic protein targets, similarly posits FBXO22 as a potential epigenetic multiplayer in human development. As mentioned above, haploinsufficiency of *KDM4B* is causal for an autosomal dominant intellectual developmental disorder (MRD65), characterized by overall delayed neurodevelopment, dysmorphic facial features, feeding difficulties, and hypotonia.[75] The overlap in neurological and additional defects in MRD65 and FBXO22-deficiency could suggest the importance of dose control of protein levels of KDM4B in neurodevelopment. Among the additional known targets of FBXO22, biallelic pathogenic variants in the homolog *KDM5B* (MIM605393) are also responsible for an autosomal recessive intellectual disorder (MRT65, MIM618109), with neurodevelopment similarly impacted, while homozygous LoF variants in *KDM5A* lead to El Hayek-Chahrour neurodevelopmental syndrome (NEDEHC, MIM620820).[76–79] This precedence, together with the wide range of likely impacted additional protein substrates of FBXO22 across multiple tissue types, could

potentially account for the neurological and the additional multi-system anomalies seen in affected individuals, warranting further exploration in organ-specific assays.

Causative variants in lysine demethylases and methyltransferases implicated in both recessive and dominant Mendelian neurological disorders have previously been associated with peripheral blood DNA methylation changes. In addition to *KDM4B* and *KDM5B* described above, epigenetic signatures have been documented for neurological disorders implicating loss of function for *KDM2B* (MIM609078), *KDM5C* (MIM314690), *KDM6A* (MIM300128), and variants associated with dominance effects for *KDM6A*, *KMT2A/B/C/D* (MIM159555, MIM606834, MIM606833, MIM602113), *KMT5B* (MIM610881), *EHMT1* (MIM607001), *SETD1B* (MIM611055) and *NSD1* (MIM606681) (further detailed in Table S4).[43–45,80] In addition, monoallelic variants in the ubiquitin ligase substrate receptor *FBXO11* with autosomal dominant inheritance (IDDFBA)[24–26] mentioned above are also marked by a DNA methylation signature (EpiSign v5). With FBXO22 molecularly implicated in regulating protein levels of several lysine demethylases and methyltransferases, likely impacting chromatin states, and with its association with neurological dysfunction, an epigenetic DNA methylation signature for *FBXO22*-deficiency, likely converging on a common methylation target (*AGAP2*) with *KMT2D*, was readily and likewise identified in peripheral blood gDNA. The *FBXO22*-deficiency peripheral blood epi-signature presents an opportunity as a biomarker for investigating the additional variants identified here, as well as future Variants of Uncertain Significance (VUS) for *FBXO22*-deficiency, while warranting further investigation into the specific molecular epigenetic pathways perturbed.

Taken together, our clinical, genetic and molecular studies define a heretofore undescribed Mendelian recessive disorder caused by homozygous *FBXO22* variants with LoF effects, characterized by multi-system anomalies and a unique epigenetic signature. This is supported by genetic and clinical data across a cohort of 14 families identifying four alleles with LoF effects, target characterization using affected fibroblasts in vitro, and epigenetic profiling with epimarker identification in peripheral blood gDNA. The ubiquitous expression of *FBXO22* coupled with the extensive repertoire of protein targets, including

epigenetic modulators, thus provides a potential underlying rationale for the pleiotropic effects of *FBXO22*-deficiency.

DATA AND CODE AVAILABILITY

The published article contains all code parameters and processed data analyzed during this study in the supplemental data. There are restrictions to the availability of raw genomic data due to IRB restrictions; enquiries on data access should be directed to the corresponding authors.

ACKNOWLEDGMENTS

We thank all the families for partaking in this study and the referring clinicians for their generous help. We thank the Genome Institute of Singapore Sequencing and Genotyping Platform for ONT-seq services in Singapore. We would also like to acknowledge the support of the Mohammed Bin Rashid University of Medicine and Health Sciences and Al Jalila Foundation. N.B.R. is a recipient of Singapore Ministry of Health's RIE2025 National Medical Research Council OF-YIRG award (OFYIRG23jan-0036; MOH-001341) administered by the Agency for Science, Technology and Research. A.A.M is a recipient of Sultan Qaboos University Strategic research funding (SR/MED/GENT/16/01). B.R. is a fellow of the Branco Weiss Foundation (Switzerland) and an EMBO Young Investigator (Europe) and the research reported in this publication was supported by funding from King Abdullah University of Science and Technology (KAUST) – KAUST Center of Excellence for Smart Health (KCSH), under award number FCC/1/5932-04-01.

AUTHOR CONTRIBUTIONS

A.A.T. and B.R. designed, conceived and supervised the study. A.M.B.-A, ascertainment, phenotype and genotype analyses of families 1 to 10; 13 to 14. S.K., N.O. and M.F. performed exome/genome sequencing data analyses and variant interpretation of families 1 to 10; 13 to 14 with supervision of J.P.B., P.B. and A.M.B.-A..

A.A.-F., A.A.-Shidhani, A.A.-M, M.Alghamdi, F.S.A., E.A.F., M.M., N.A.M.A., A.A.Shamsi, G.E., H.A.S., M.A.O., A.W.E.-H., S.A.S.A.-K., N.A., F.A., A.A.Saman, H.T., M.Arabi, S.K., A.T., M.Alfadhel, R.J., S.Shenbagam, M.E.B., A.J., N.T., F.R., I.C., M.A.A. and A.A.-A.

were involved in conducting the clinical and genetic evaluation of the affected individuals, organisation of clinical information, the collection of human biological samples and the whole genome/exome sequencing for the affected families. U.A. reviewed facial findings to evaluate dysmorphic features and contributed to the writing of the relevant part of the article. N.B.R., Y.J., N.A.A., U.B.M.S., A.A.T., S.Sinha, R.R. and A.P. performed experimental work, formal data analysis and visualisation with supervision from F.R.A., T.O., M.N., A.A.T. and B.R.. N.B.R., A.A.T. and B.R. wrote and edited the manuscript. N.B.R., J.W.S., F.R.A., A.M.B.-A, A.A.T. and B.R. provided resources and acquired funding.

DECLARATION OF INTERESTS

P.B., S.K., N.O., M.F., J.P.B. and A.M.B.-A. are employees of Centogene GmbH. All other authors declare no conflicts of interest.

WEB RESOURCES

The following web resources were used in this study: The Online Mendelian Inheritance in Man (OMIM): http://www.omim.org ; The Exome Variant Server (ftp://ftp.ncbi.nlm.nih.gov/pub/clinvar/vcf_GRCh37) from NHLBI Exome Sequencing Project (ESP): http://evs.gs.washington.edu/EVS/ ; 1000 Genome Project Database: http://browser.1000genomes.org/index.html ; Genome Aggregation Database (GnomAD v4.1.0 (hg38) and v2.1.1 (hg19)): http://gnomad.broadinstitute.org/ ; BRAVO/TOPmed database: (https://bravo.sph.umich.edu/freeze8/hg38/); Greater Middle East (GME) Variome web: http://igm.ucsd.edu/gme/index.php ; NCBI dbSNP: http://www.ncbi.nlm.nih.gov/SNP/ ; DECIPHER database (GRCh38, v11.27): https://www.deciphergenomics.org ; PheWAS catalog: https://phewascatalog.org/phewas ; NHGRI-EBI GWAS catalog (GRCh38.p14 amd dbSNP build 156): https://www.ebi.ac.uk/gwas/ ; BioGRID ORCS v1.1.16.1: https://orcs.thebiogrid.org ; WHO Anthro Survey Analyser (https://worldhealthorg.shinyapps.io/anthro/) ; BioRender (https://BioRender.com/h26g880.)

FIGURE LEGENDS AND TABLES

Figure 1. Predicted biallelic *FBXO22* variants with loss-of-function effects in 16 cases with multi-system anomalies. (A) Pedigrees of 14 families segregating autosomal recessive congenital multi-system anomalies. Crossed symbols indicate deceased individuals. Crossed triangular symbols indicate Termination of Pregnancy (TOP) and triangular symbols indicate miscarriage. Germline *FBXO22* variant coordinates are indicated below the pedigrees, colored by variant. Note that the deceased individual F13-II:1 was flagged on hindsight and not fully phenotyped and not sequenced, thus not included in the tally (see Supplementary Case Reports). (B) Facial images of five affected individuals (top row), and timelapse facial images of individuals F2-II:3 from two months to 12 years of age (bottom row, left) and F7-II:3 from eight months to 3 years of age (bottom row, right). Individual IDs colored by variant. (C) Images of hands and feet featuring the tapering digits of affected individuals F2-II:3 and F7-II:1, with IDs colored by variant. (D) Minor allele frequency (x-axis) and scaled-CADD score (y-axis) of homozygous *FBXO22* coding variants found in gnomAD v.4.0.1 (grey dots, n = 37) and those found in each of the 14 families coloured by variant (n = 4).

Figure 2. Loss of FBXO22 in affected primary fibroblasts leads to abnormally high KDM4B levels. (A) Schematic diagram of the genomic (top) and protein (bottom) structure of FBXO22 in humans. FBXO22 contains two conserved domains: F-Box (green) and the FIST domain subdivided into three sub-domains (the protein schematic is color coded by domain). The four homozygous genetic variants and corresponding protein mutations are indicated. The variants are color coded to match Figure 1. (B-C) *FBXO22* expression and FBXO22 levels analysis in primary dermal cutaneous fibroblasts from F7-II:3 with control (WT). (B) *FBXO22* expression levels normalised to housekeeping *ACTB* expression levels, relative to the WT control (n = 3 biological/experimental replicates), with significant reduction in *FBXO22* levels. ****p = 0.0000295 (unpaired, two-way student's t-test). (C) Representative western blot of endogenous FBXO22 with ACTB as the housekeeping control, showing negligible FBXO22 levels in the affected fibroblasts. (D) *FBXO22* mRNA levels in affected primary fibroblasts normalised to housekeeping *ACTB* and *GAPDH* mRNA levels, relative to the WT control with

cycloheximide (CHX) treatment at 0 and 24 hours (n = 3 biological/experimental replicates), with significant increase in *FBXO22* levels for affected cells. *p = 0.0336; ns, nonsignificant (two-way ANOVA with Fisher's Least Significant Difference multiple comparison test). (E, F) *KDM4B* expression and KDM4B accumulation analysis in primary dermal cutaneous fibroblasts from F7-II:3 with WT. (E) *KDM4B* expression levels normalised to housekeeping *ACTB* expression levels, relative to the WT control (n = 3 biological/experimental replicates). ns, nonsignificant (unpaired, two-way student's t-test). (F) Representative Western blot of endogenous KDM4B levels with ACTB as the housekeeping control, showing increased KDM4B levels in the affected fibroblasts. (G) *FLAG-HA-FBXO22* mRNA levels in HEK293T cells 48h after overexpression of *GFP* as control, and *FLAG-HA-FBXO22* WT and p.Val222del constructs. ND, not detected; ns, nonsignificant (unpaired, two-way student's t-test). (H) Representative Western blot of FLAG-HA-FBXO22 constructs (anti-FLAG) from HEK293T cells 48h after transfection, with GAPDH as the housekeeping control. (H′) Quantification of FLAG-HA-FBXO22 levels from Western blots from panel H, normalised to GAPDH levels and relative to WT controls (n = 3 biological/experimental replicates). *p = 0.0275 (unpaired, two-way student's t-test).

Figure 3. Loss of *FBXO22* is associated with a unique epigenetic signature in peripheral blood (A) Heatmap with euclidean distance hierarchical clustering of DNA methylation values for the top 40 differentially-methylated regions featuring the *FBXO22* epi-signature for three *FBXO22*-deficiency peripheral blood samples integrated with the 34 EpiSign Mendelian neurodevelopmental disorders (MNDD-cohort) and control dataset. See Table S4 for EpiSign syndrome acronym definitions. The variant is color coded to match Figure 1. (B) Principal component analysis on the 40 regions representing the DNA methylation epi-signature in PBMCs of three affected individuals lacking *FBXO22* showing clustering of all three samples away from the EpiSign MNDD-cohort and control. Variance explained by components PC1 and PC2 are indicated in brackets. (C) Genome browser view of the differentially methylated (orange) region of the 3′-UTR within the ultimate exon 19 of *AGAP2* featuring aggregated CpG methylation (5mC - red; unmodified C - blue) of ONT-seq long reads from the three *FBXO22*-deficiency samples and three samples from the separate set of general neurological disorders (ND-cohort).

(D) Methylation values at the differentially methylated probed region within the 3′-UTR of *AGAP2* in the *FBXO22*-deficiency ONT-seq samples (n=3), ND-cohort ONT-seq samples (n=17, p=0.013) and EpiSign MNDD-cohort samples (n=34, p=0.015). Error bars denote SD. *p < 0.05; ns, non-significant (unpaired, two-way student's t-test).

Table 1. Summary of key clinical data of 15 affected individuals with biallelic *FBXO22* LoF variants.

Key clinical feature of *FBXO22* deficient individuals	Standardized Human Phenotype Ontology	Penetrance
Total number of affected individuals		15[a]
Growth		
Failure to thrive	HP:0001508	86.7%
Intrauterine growth restriction	HP:0001511	73.3%
Short stature	HP:0004322	66.7%
Decreased body weight	HP:0004325	60.0%
Neurodevelopment		
Neurodevelopmental delay	HP:0012758	86.7%
Microcephaly	HP:0011451	73.3%
Muscular hypotonia	HP:0001252	66.7%
Seizures	HP:0001250	53.3%
Generalized hypotonia	HP:0001290	53.3%
Intellectual disability	HP:0001249	46.7%
Poor suck	HP:0002033	40.0%
Craniofacial		
Abnormal craniofacial shape	HP:0001999	80.0%
Depressed nasal bridge	HP:0005280	60.0%
High forehead	HP:0000348	53.3%
Hypertelorism	HP:0000316	46.7%

[a]Excluding fetal case (F4-II:3) where full phenotyping was not possible.

Table 2. Expression profiles and associated diseases of genes with promoter or proximal DNA methylation differences with phenotypic relevance within the differentially-methylated regions of *FBXO22*-deficiency, ranked from most hypomethylated to most hypermethylated

Gene	Methylation Call	Expression	Associated diseases
LY6G6D	Hypomethylated	Skin – GI tract	Anemia, Nonspherocytic Hemolytic
MEOX1	Hypomethylated	Heart – Adipose tissue	Klippel-Feil syndrome
SLC22A23	Hypomethylated	Brain - Parathyroid gland – GI tract	Wolf-Hirschhorn Syndrome Inflammatory Bowel Disease
MYH7B	Hypomethylated	Heart – Skeletal muscles	Cardiomyopathy
AGAP2	Hypomethylated	Brain	Kabuki Syndrome
TRMT9B	Hypomethylated	Brain – Thyroid	Dubowitz syndrome
GALNT9	Hypomethylated	Brain – Thyroid – Kidney	Association with autism spectrum disorders and Parkinson's disease
ARHGEF10	Hypomethylated	Brain – Lungs – Heart – Skeletal muscle	Slowed Nerve Conduction Velocity (SNCV) Axonal neuropathy
PRDM16	Hypomethylated	GI tract – Thyroid – Brain – Kidney – Heart	Cardiomyopathy
ZNF385A	Hypomethylated	Brain – Skin – Retina	Encephalopathy Cone-Rod Dystrophy 2
DDR1	Hypomethylated	Brian – Skin – GI tract – Kidneys	Spondylo-meta-epiphyseal dysplasia
NAT8L	Hypomethylated	Brain – Lungs – Retina – Adipose tissue – Pituitary gland – Skeletal muscle	N-acetylaspartate deficiency Cardiomyopathy Neurodegeneration Alzheimer
TRIM15	Hypomethylated	GI tract – Liver – Kidneys – Colon	Hepatic veno-occlusive disease with immunodeficiency
DDX39B	Hypomethylated	Brain – Thyroid – Bone marrow – Kidneys – Lungs – Skin – Heart – Skeletal muscle	Neurodevelopmental delay Epilepsy Short stature and congenital hypotonia Anterior horn cell
TAPBP	Hypomethylated	Liver – Bone marrow – Brain – Heart	Bare lymphocyte syndrome
MED13	Hypomethylated	Bone marrow – Liver – Lungs – Retina	MRFACD syndrome
OLIG1	Hypomethylated	Brain	Oligodendroglioma
MPIG6B	Hypermethylated	Lungs – Skin – Spleen	Congenital macrothrombocytopenia with focal myelofibrosis
DDAH2	Hypermethylated	Heart – Lungs – Thyroid - GI tract – Kidneys	Coronary artery disease
SLC17A5	Hypermethylated	Parathyroid gland – Retina – Liver	Salla disease Free Sialic Acid Storage Disorders

References

1. Ciechanover, A., and Schwartz, A.L. (1998). The ubiquitin-proteasome pathway: The complexity and myriad functions of proteins death. Proc. Natl. Acad. Sci. *95*, 2727–2730. https://doi.org/10.1073/pnas.95.6.2727.

2. Ciechanover, A. (2005). Proteolysis: from the lysosome to ubiquitin and the proteasome. Nat. Rev. Mol. Cell Biol. 6, 79–87. https://doi.org/10.1038/nrm1552.

3. Finley, D. (2009). Recognition and Processing of Ubiquitin-Protein Conjugates by the Proteasome. Biochemistry *78*, 477–513. https://doi.org/10.1146/annurev.biochem.78.081507.101607.

4. Senft, D., Qi, J., and Ronai, Z.A. (2018). Ubiquitin ligases in oncogenic transformation and cancer therapy. Nat. Rev. Cancer 18, 69–88. https://doi.org/10.1038/nrc.2017.105.

5. George, A.J., Hoffiz, Y.C., Charles, A.J., Zhu, Y., and Mabb, A.M. (2018). A Comprehensive Atlas of E3 Ubiquitin Ligase Mutations in Neurological Disorders. Front. Genet. 9, 29. https://doi.org/10.3389/fgene.2018.00029.

6. Meroni, G. (2020). Proteostasis and Disease, From Basic Mechanisms to Clinics. Adv. Exp. Med. Biol. *1233*, 311–325. https://doi.org/10.1007/978-3-030-38266-7_14.

7. Duan, S., and Pagano, M. (2021). Ubiquitin ligases in cancer: Functions and clinical potentials. Cell Chem. Biol. *28*, 918–933. https://doi.org/10.1016/j.chembiol.2021.04.008.

8. Craig, K.L., and Tyers, M. (1999). The F-box: a new motif for ubiquitin dependent proteolysis in cell cycle regulation and signal transduction. Prog. Biophys. Mol. Biol. 72, 299–328. https://doi.org/10.1016/s0079-6107(99)00010-3.

9. Kipreos, E.T., and Pagano, M. (2000). The F-box protein family. Genome Biol. 1, reviews3002.1. https://doi.org/10.1186/gb-2000-1-5-reviews3002.

10. Nguyen, K.M., and Busino, L. (2020). Cullin-RING Ligases and Protein Neddylation, Biology and Therapeutics. Adv. Exp. Med. Biol. *1217*, 111–122. https://doi.org/10.1007/978-981-15-1025-0_8.

11. Yumimoto, K., Yamauchi, Y., and Nakayama, K.I. (2020). F-Box Proteins and Cancer. Cancers 12, 1249. https://doi.org/10.3390/cancers12051249.

12. Cheng, J., Lin, M., Chu, M., Gong, L., Bi, Y., and Zhao, Y. (2020). Emerging role of

FBXO22 in carcinogenesis. Cell Death Discov 6, 66. https://doi.org/10.1038/s41420-020-00303-0.

13. Johmura, Y., Harris, A.S., Ohta, T., and Nakanishi, M. (2020). FBXO22, an epigenetic multiplayer coordinating senescence, hormone signaling, and metastasis. Cancer Sci 111, 2718–2725. https://doi.org/10.1111/cas.14534.

14. Johmura, Y., Sun, J., Kitagawa, K., Nakanishi, K., Kuno, T., Naiki-Ito, A., Sawada, Y., Miyamoto, T., Okabe, A., Aburatani, H., et al. (2016). SCFFbxo22-KDM4A targets methylated p53 for degradation and regulates senescence. Nat Commun 7, 10574. https://doi.org/10.1038/ncomms10574.

15. Ge, M.-K., Zhang, N., Xia, L., Zhang, C., Dong, S.-S., Li, Z.-M., Ji, Y., Zheng, M.-H., Sun, J., Chen, G.-Q., et al. (2020). FBXO22 degrades nuclear PTEN to promote tumorigenesis. Nat Commun 11, 1720. https://doi.org/10.1038/s41467-020-15578-1.

16. Li, S., He, J., Liao, X., He, Y., Chen, R., Chen, J., Hu, S., and Sun, J. (2022). Fbxo22 inhibits metastasis in triple-negative breast cancer through ubiquitin modification of KDM5A and regulation of H3K4me3 demethylation. Cell Biol Toxicol, 1–15. https://doi.org/10.1007/s10565-022-09754-w.

17. Lin, M., Zhang, J., Bouamar, H., Wang, Z., Sun, L.-Z., and Zhu, X. (2022). Fbxo22 promotes cervical cancer progression via targeting p57Kip2 for ubiquitination and degradation. Cell Death Dis 13, 805. https://doi.org/10.1038/s41419-022-05248-z.

18. Tan, M.-K.M., Lim, H.-J., and Harper, J.W. (2011). SCF FBXO22 Regulates Histone H3 Lysine 9 and 36 Methylation Levels by Targeting Histone Demethylase KDM4A for Ubiquitin-Mediated Proteasomal Degradation. Mol Cell Biol 31, 3687–3699. https://doi.org/10.1128/mcb.05746-11.

19. Johmura, Y., Maeda, I., Suzuki, N., Wu, W., Goda, A., Morita, M., Yamaguchi, K., Yamamoto, M., Nagasawa, S., Kojima, Y., et al. (2018). Fbxo22-mediated KDM4B degradation determines selective estrogen receptor modulator activity in breast cancer. J Clin Invest 128, 5603–5619. https://doi.org/10.1172/jci121679.

20. Tian, X., Dai, S., Sun, J., Jin, G., Jiang, S., Meng, F., Li, Y., Wu, D., and Jiang, Y. (2015). F-box protein FBXO22 mediates polyubiquitination and degradation of KLF4 to promote hepatocellular carcinoma progression. Oncotarget 6, 22767–22775. https://doi.org/10.18632/oncotarget.4082.

21. Yoo, D., Choi, J.-H., Im, J.-H., Kim, M.J., Kim, H.-J., Park, S.S., and Jeon, B. (2020). Young-Onset Parkinson's Disease with Impulse Control Disorder Due to Novel Variants of F-Box Only Protein 7. J. Mov. Disord. 13, 225–228. https://doi.org/10.14802/jmd.20026.

22. Shojaee, S., Sina, F., Banihosseini, S.S., Kazemi, M.H., Kalhor, R., Shahidi, G.-A., Fakhrai-Rad, H., Ronaghi, M., and Elahi, E. (2008). Genome-wide Linkage Analysis of a Parkinsonian-Pyramidal Syndrome Pedigree by 500 K SNP Arrays. Am. J. Hum. Genet. 82, *137*5–1384. https://doi.org/10.1016/j.ajhg.2008.05.005.

23. Fonzo, A.D., Dekker, M.C.J., Montagna, P., Baruzzi, A., Yonova, E.H., Guedes, L.C., Szczerbinska, A., Zhao, T., Dubbel-Hulsman, L.O.M., Wouters, C.H., et al. (2009). FBXO7 mutations cause autosomal recessive, early-onset parkinsonian-pyramidal syndromeSYMBOL. Neurology 72, 240–245. https://doi.org/10.1212/01.wnl.0000338144.10967.2b.

24. Fritzen, D., Kuechler, A., Grimmel, M., Becker, J., Peters, S., Sturm, M., Hundertmark, H., Schmidt, A., Kreiß, M., Strom, T.M., et al. (2018). De novo FBXO11 mutations are associated with intellectual disability and behavioural anomalies. Hum. Genet. 137, 401–411. https://doi.org/10.1007/s00439-018-1892-1.

25. Gregor, A., Sadleir, L.G., Asadollahi, R., Azzarello-Burri, S., Battaglia, A., Ousager, L.B., Boonsawat, P., Bruel, A.-L., Buchert, R., Calpena, E., et al. (2018). De Novo Variants in the F-Box Protein FBXO11 in 20 Individuals with a Variable Neurodevelopmental Disorder. Am. J. Hum. Genet. 103, 305–316. https://doi.org/10.1016/j.ajhg.2018.07.003.

26. Jansen, S., Werf, I.M. van der, Innes, A.M., Afenjar, A., Agrawal, P.B., Anderson, I.J., Atwal, P.S., Binsbergen, E. van, Boogaard, M.-J. van den, Castiglia, L., et al. (2019). De novo variants in FBXO11 cause a syndromic form of intellectual disability with behavioral problems and dysmorphisms. Eur. J. Hum. Genet. 27, 738–746. https://doi.org/10.1038/s41431-018-0292-2.

27. Mir, A., Sritharan, K., Mittal, K., Vasli, N., Araujo, C., Jamil, T., Rafiq, M.A., Anwar, Z., Mikhailov, A., Rauf, S., et al. (2014). Truncation of the E3 ubiquitin ligase component FBXO31 causes non-syndromic autosomal recessive intellectual disability in a Pakistani family. Hum. Genet. *133*, 975–984. https://doi.org/10.1007/s00439-014-1438-0.

28. Borziak, K., and Zhulin, I.B. (2007). FIST: a sensory domain for diverse signal transduction pathways in prokaryotes and ubiquitin signaling in eukaryotes. Bioinformatics 23, 2518–2521. https://doi.org/10.1093/bioinformatics/btm384.

29. Goretzki, B., Khoshouei, M., Schröder, M., Penner, P., Egger, L., Stephan, C., Argoti, D., Dierlamm, N., Rada, J.M., Kapps, S., et al. (2024). Dual BACH1 regulation by complementary SCF-type E3 ligases. Cell. https://doi.org/10.1016/j.cell.2024.11.006.

30. Cao, S., Garcia, S.F., Shi, H., James, E.I., Kito, Y., Shi, H., Mao, H., Kaisari, S., Rona, G., Deng, S., et al. (2024). Recognition of BACH1 quaternary structure degrons by two F-box proteins under oxidative stress. Cell. https://doi.org/10.1016/j.cell.2024.10.012.

31. Schwarz, J.M., Rödelsperger, C., Schuelke, M., and Seelow, D. (2010). MutationTaster evaluates disease-causing potential of sequence alterations. Nat. Methods 7, 575–576. https://doi.org/10.1038/nmeth0810-575.

32. Kurosaki, T., and Maquat, L.E. (2016). Nonsense-mediated mRNA decay in humans at a glance. J. Cell Sci. *129*, 461–467. https://doi.org/10.1242/jcs.181008.

33. Hug, N., Longman, D., and Cáceres, J.F. (2016). Mechanism and regulation of the nonsense-mediated decay pathway. Nucleic Acids Res. 44, 1483–1495. https://doi.org/10.1093/nar/gkw010.

34. Supek, F., Lehner, B., and Lindeboom, R.G.H. (2021). To NMD or Not To NMD: Nonsense-Mediated mRNA Decay in Cancer and Other Genetic Diseases. Trends Genet. 37, 657–668. https://doi.org/10.1016/j.tig.2020.11.002.

35. Lindeboom, R.G.H., Vermeulen, M., Lehner, B., and Supek, F. (2019). The impact of nonsense-mediated mRNA decay on genetic disease, gene editing and cancer immunotherapy. Nat. Genet. 51, 1645–1651. https://doi.org/10.1038/s41588-019-0517-5.

36. Lindeboom, R.G.H., Supek, F., and Lehner, B. (2016). The rules and impact of nonsense-mediated mRNA decay in human cancers. Nat. Genet. 48, 1112–1118. https://doi.org/10.1038/ng.3664.

37. Abramson, J., Adler, J., Dunger, J., Evans, R., Green, T., Pritzel, A., Ronneberger, O., Willmore, L., Ballard, A.J., Bambrick, J., et al. (2024). Accurate structure prediction of biomolecular interactions with AlphaFold 3. Nature, 1–3. https://doi.org/10.1038/s41586-024-07487-w.

38. Woods, H., Schiano, D.L., Aguirre, J.I., Ledwitch, K.V., McDonald, E.F., Voehler, M., Meiler, J., and Schoeder, C.T. (2023). Computational modeling and prediction of deletion

mutants. Structure 31, 713-723.e3. https://doi.org/10.1016/j.str.2023.04.005.

39. Almarri, M.A., Haber, M., Lootah, R.A., Hallast, P., Turki, S.A., Martin, H.C., Xue, Y., and Tyler-Smith, C. (2021). The genomic history of the Middle East. Cell *184*, 4612-4625.e14. https://doi.org/10.1016/j.cell.2021.07.013.

40. Cetinkaya, A., Xiong, J.R., Vargel, İ., Kösemehmetoğlu, K., Canter, H.İ., Gerdan, Ö.F., Longo, N., Alzahrani, A., Camps, M.P., Taskiran, E.Z., et al. (2016). Loss-of-Function Mutations in ELMO2 Cause Intraosseous Vascular Malformation by Impeding RAC1 Signaling. Am. J. Hum. Genet. 99, 299–317. https://doi.org/10.1016/j.ajhg.2016.06.008.

41. Wilson, C., and Krieg, A.J. (2019). KDM4B: A Nail for Every Hammer? Genes 10, 134. https://doi.org/10.3390/genes10020134.

42. Wang, Z., Cai, H., Zhao, E., and Cui, H. (2022). The Diverse Roles of Histone Demethylase KDM4B in Normal and Cancer Development and Progression. Front. Cell Dev. Biol. 9, 790129. https://doi.org/10.3389/fcell.2021.790129.

43. Rooney, K., and Sadikovic, B. (2022). DNA Methylation Episignatures in Neurodevelopmental Disorders Associated with Large Structural Copy Number Variants: Clinical Implications. Int. J. Mol. Sci. 23, 7862. https://doi.org/10.3390/ijms23147862.

44. Levy, M.A., Relator, R., McConkey, H., Pranckeviciene, E., Kerkhof, J., Barat- Houari, M., Bargiacchi, S., Biamino, E., Bralo, M.P., Cappuccio, G., et al. (2022). Functional correlation of genome- wide DNA methylation profiles in genetic neurodevelopmental disorders. Hum. Mutat. 43, 1609–1628. https://doi.org/10.1002/humu.24446.

45. Levy, M.A., McConkey, H., Kerkhof, J., Barat-Houari, M., Bargiacchi, S., Biamino, E., Bralo, M.P., Cappuccio, G., Ciolfi, A., Clarke, A., et al. (2022). Novel diagnostic DNA methylation episignatures expand and refine the epigenetic landscapes of Mendelian disorders. Hum. Genet. Genom. Adv. 3, 100075. https://doi.org/10.1016/j.xhgg.2021.100075.

46. Bannister, A.J., and Kouzarides, T. (2011). Regulation of chromatin by histone modifications. Cell Res. 21, 381–395. https://doi.org/10.1038/cr.2011.22.

47. Cedar, H., and Bergman, Y. (2009). Linking DNA methylation and histone modification: patterns and paradigms. Nat. Rev. Genet. 10, 295–304. https://doi.org/10.1038/nrg2540.

48. Klose, R.J., and Zhang, Y. (2007). Regulation of histone methylation by demethylimination and demethylation. Nat. Rev. Mol. Cell Biol. 8, 307–318. https://doi.org/10.1038/nrm2143.

49. Lehnertz, B., Ueda, Y., Derijck, A.A.H.A., Braunschweig, U., Perez-Burgos, L., Kubicek, S., Chen, T., Li, E., Jenuwein, T., and Peters, A.H.F.M. (2003). Suv39h-Mediated Histone H3 Lysine 9 Methylation Directs DNA Methylation to Major Satellite Repeats at Pericentric Heterochromatin. Curr. Biol. 13, *119*2–1200. https://doi.org/10.1016/s0960-9822(03)00432-9.

50. Aref-Eshghi, E., Kerkhof, J., Pedro, V.P., France, G.D., Barat-Houari, M., Ruiz-Pallares, N., Andrau, J.-C., Lacombe, D., Van-Gils, J., Fergelot, P., et al. (2020). Evaluation of DNA Methylation Episignatures for Diagnosis and Phenotype Correlations in 42 Mendelian Neurodevelopmental Disorders. Am J Hum Genetics *106*, 356–370. https://doi.org/10.1016/j.ajhg.2020.01.019.

51. Sinha, S., Rabea, F., Ramaswamy, S., Chekroun, I., Naofal, M.E., Jain, R., Alfalasi, R., Halabi, N., Yaslam, S., Hassani, M.S., et al. (2025). Long read sequencing enhances pathogenic and novel variation discovery in patients with rare diseases. Nat. Commun. *16*, 2500. https://doi.org/10.1038/s41467-025-57695-9.

52. Nitta, A., Noike, H., Sumi, K., Miyanishi, H., Tanaka, T., Takaoka, K., Nagakura, M., Iegaki, N., Kaji, J., Miyamoto, Y., et al. (2018). Nicotinic Acetylcholine Receptor Signaling in Neuroprotection. 89–111. https://doi.org/10.1007/978-981-10-8488-1_6.

53. Booth, K.T.A., Jangam, S.V., Chui, M.M.C., Treat, K., Graziani, L., Soldano, A., White, K., Christensen, C.K., Lynnes, T., Yamamoto, S., et al. (2023). De novo and inherited variants in DDX39B cause a Novel Syndrome Characterized by Neurodevelopmental Delay, Short Stature, and Congenital Hypotonia. medRxiv, 2023.07.15.23292630. https://doi.org/10.1101/2023.07.15.23292630.

54. Dwyer, C.A., and Esko, J.D. (2016). Glycan susceptibility factors in autism spectrum disorders. Mol. Asp. Med. 51, 104–114. https://doi.org/10.1016/j.mam.2016.07.001.

55. Trivisano, M., Dominicis, A.D., Micalizzi, A., Ferretti, A., Dentici, M.L., Terracciano, A., Calabrese, C., Vigevano, F., Novelli, G., Novelli, A., et al. (2022). MED13 mutation: A novel cause of developmental and epileptic encephalopathy with infantile spasms. Seizure 101, 211–217. https://doi.org/10.1016/j.seizure.2022.09.002.

56. Szu, J., Wojcinski, A., Jiang, P., and Kesari, S. (2021). Impact of the Olig Family on

Neurodevelopmental Disorders. Front. Neurosci. 15, 659601. https://doi.org/10.3389/fnins.2021.659601.

57. Kühnisch, J., Theisen, S., Dartsch, J., Fritsche-Guenther, R., Kirchner, M., Obermayer, B., Bauer, A., Kahlert, A.-K., Rothe, M., Beule, D., et al. (2023). Prdm16 mutation determines sex-specific cardiac metabolism and identifies two novel cardiac metabolic regulators. Cardiovasc. Res. 119, 2902–2916. https://doi.org/10.1093/cvr/cvad154.

58. Chen, P., Li, Z., Nie, J., Wang, H., Yu, B., Wen, Z., Sun, Y., Shi, X., Jin, L., and Wang, D.-W. (2020). MYH7B variants cause hypertrophic cardiomyopathy by activating the CaMK-signaling pathway. Sci. China Life Sci. 63, 1347–1362. https://doi.org/10.1007/s11427-019-1627-y.

59. Bayrakli, F., Guclu, B., Yakicier, C., Balaban, H., Kartal, U., Erguner, B., Sagiroglu, M.S., Yuksel, S., Ozturk, A.R., Kazanci, B., et al. (2013). Mutation in MEOX1 gene causes a recessive Klippel-Feil syndrome subtype. BMC Genet. 14, 95–95. https://doi.org/10.1186/1471-2156-14-95.

60. Aref-Eshghi, E., Schenkel, L.C., Lin, H., Skinner, C., Ainsworth, P., Paré, G., Rodenhiser, D., Schwartz, C., and Sadikovic, B. (2017). The defining DNA methylation signature of Kabuki syndrome enables functional assessment of genetic variants of unknown clinical significance. Epigenetics 12, 923–933. https://doi.org/10.1080/15592294.2017.1381807.

61. Jung, Y.L., Hung, C., Choi, J., Lee, E.A., and Bodamer, O. (2023). Characterizing the molecular impact of KMT2D variants on the epigenetic and transcriptional landscapes in Kabuki syndrome. Hum. Mol. Genet. 32, 2251–2261. https://doi.org/10.1093/hmg/ddad059.

62. Haczynski, J., Tarkowski, R., Jarzabek, K., Slomczynska, M., Wolczynski, S., Magoffin, D., Jakowicki, J., and Jakimiuk, A. (2002). Human cultured skin fibroblasts express estrogen receptor α and β. Int. J. Mol. Med. https://doi.org/10.3892/ijmm.10.2.149.

63. Zhang, L., Chen, J., Ning, D., Liu, Q., Wang, C., Zhang, Z., Chu, L., Yu, C., Liang, H., Zhang, B., et al. (2019). FBXO22 promotes the development of hepatocellular carcinoma by regulating the ubiquitination and degradation of p21. J Exp Clin Canc Res 38, 101. https://doi.org/10.1186/s13046-019-1058-6.

64. Zhu, X.-N., He, P., Zhang, L., Yang, S., Zhang, H.-L., Zhu, D., Liu, M.-D., and Yu, Y. (2019). FBXO22 mediates polyubiquitination and inactivation of LKB1 to promote lung cancer cell growth. Cell Death Dis 10, 486. https://doi.org/10.1038/s41419-019-1732-9.

65. Bai, J., Wu, K., Cao, M.-H., Yang, Y., Pan, Y., Liu, H., He, Y., Itahana, Y., Huang, L., Zheng, J.-N., et al. (2019). SCFFBXO22 targets HDM2 for degradation and modulates breast cancer cell invasion and metastasis. Proc. Natl. Acad. Sci. *116*, 11754–11763. https://doi.org/10.1073/pnas.1820990116.

66. De, S., Holvey-Bates, E.G., Mahen, K., Willard, B., and Stark, G.R. (2021). The ubiquitin E3 ligase FBXO22 degrades PD-L1 and sensitizes cancer cells to DNA damage. Proc. Natl. Acad. Sci. 118, e2112674118. https://doi.org/10.1073/pnas.2112674118.

67. Wu, B., Liu, Z.-Y., Cui, J., Yang, X.-M., Jing, L., Zhou, Y., Chen, Z.-N., and Jiang, J.-L. (2017). F-Box Protein FBXO22 Mediates Polyubiquitination and Degradation of CD147 to Reverse Cisplatin Resistance of Tumor Cells. Int. J. Mol. Sci. 18, 212. https://doi.org/10.3390/ijms18010212.

68. Basu, A.A., Zhang, C., Riha, I.A., Magassa, A., Ko, F., and Zhang, X. (2023). A CRISPR activation screen identifies FBXO22 as an E3 ligase supporting targeted protein degradation. bioRxiv, 2023.09.15.557708. https://doi.org/10.1101/2023.09.15.557708.

69. Zhu, X.-N., Wei, Y.-S., Yang, Q., Liu, H.-R., Zhi, Z., Zhu, D., Xia, L., Hong, D.-L., Yu, Y., and Chen, G.-Q. (2023). FBXO22 promotes leukemogenesis by targeting BACH1 in MLL-rearranged acute myeloid leukemia. J. Hematol. Oncol. 16, 9. https://doi.org/10.1186/s13045-023-01400-0.

70. Liu, L., Matsumoto, M., Matsui-Watanabe, M., Nakagawa, T., Nagasawa, Y., Pang, J., Callens, B.K.K., Muto, A., Ochiai, K., Takekawa, H., et al. (2024). TANK binding kinase 1 promotes BACH1 degradation through both phosphorylation-dependent and -independent mechanisms without relying on heme and FBXO22. bioRxiv, 2024.02.15.580587. https://doi.org/10.1101/2024.02.15.580587.

71. Lei, Z., Luo, Y., Fu, Q., Lu, J., Wang, C., Zhang, L., and Zhang, Z. (2025). Ribosomal protein L6 suppresses hepatocellular carcinoma by modulating FBXO22-mediated p53 degradation. Cell. Signal. *127*, 111612. https://doi.org/10.1016/j.cellsig.2025.111612.

72. Watanabe-Matsui, M., Kadoya, S., Segawa, K., Shima, H., Nakagawa, T., Nagasawa, Y., Hayashi, S., Matsumoto, M., Ikeda, M., Muto, A., et al. (2025). Heme regulates protein interactions and phosphorylation of BACH2 intrinsically disordered region in humoral

response. iScience 28, 111529. https://doi.org/10.1016/j.isci.2024.111529.

73. Ge, M.-K., Zhang, C., Zhang, N., He, P., Cai, H.-Y., Li, S., Wu, S., Chu, X.-L., Zhang, Y.-X., Ma, H.-M., et al. (2023). The tRNA-GCN2-FBXO22-axis-mediated mTOR ubiquitination senses amino acid insufficiency. Cell Metab. https://doi.org/10.1016/j.cmet.2023.10.016.

74. Dai, X., Yan, P., and Wei, W. (2023). Amino acid availability governs mTOR ubiquitination. Cell Res., 1–2. https://doi.org/10.1038/s41422-023-00910-3.

75. Duncan, A.R., Vitobello, A., Collins, S.C., Vancollie, V.E., Lelliott, C.J., Rodan, L., Shi, J., Seman, A.R., Agolini, E., Novelli, A., et al. (2020). Heterozygous Variants in KDM4B Lead to Global Developmental Delay and Neuroanatomical Defects. Am. J. Hum. Genet. 107, 1170–1177. https://doi.org/10.1016/j.ajhg.2020.11.001.

76. Albert, M., Schmitz, S.U., Kooistra, S.M., Malatesta, M., Torres, C.M., Rekling, J.C., Johansen, J.V., Abarrategui, I., and Helin, K. (2013). The Histone Demethylase Jarid1b Ensures Faithful Mouse Development by Protecting Developmental Genes from Aberrant H3K4me3. PLoS Genet. 9, e1003461. https://doi.org/10.1371/journal.pgen.1003461.

77. Martin, H.C., Jones, W.D., McIntyre, R., Sanchez-Andrade, G., Sanderson, M., Stephenson, J.D., Jones, C.P., Handsaker, J., Gallone, G., Bruntraeger, M., et al. (2018). Quantifying the contribution of recessive coding variation to developmental disorders. Science 362, 1161–1164. https://doi.org/10.1126/science.aar6731.

78. Faundes, V., Newman, W.G., Bernardini, L., Canham, N., Clayton-Smith, J., Dallapiccola, B., Davies, S.J., Demos, M.K., Goldman, A., Gill, H., et al. (2018). Histone Lysine Methylases and Demethylases in the Landscape of Human Developmental Disorders. Am. J. Hum. Genet. 102, 175–187. https://doi.org/10.1016/j.ajhg.2017.11.013.

79. Hayek, L.E., Tuncay, I.O., Nijem, N., Russell, J., Ludwig, S., Kaur, K., Li, X., Anderton, P., Tang, M., Gerard, A., et al. (2020). KDM5A mutations identified in autism spectrum disorder using forward genetics. eLife 9, e56883. https://doi.org/10.7554/elife.56883.

80. Jaarsveld, R.H. van, Reilly, J., Cornips, M.-C., Hadders, M.A., Agolini, E., Ahimaz, P., Anyane-Yeboa, K., Bellanger, S.A., Binsbergen, E. van, Boogaard, M.-J. van den, et al. (2023). Delineation of a KDM2B-related neurodevelopmental disorder and its associated DNA methylation signature. Genet Med 25, 49–62. https://doi.org/10.1016/j.gim.2022.09.006.

Figure 1

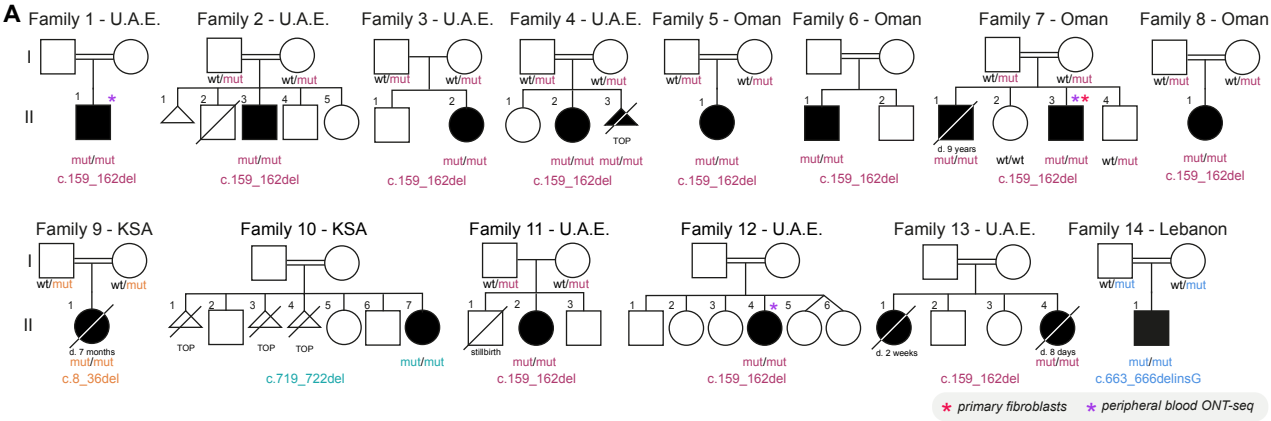
A
Family 1 - U.A.E.
Family 2 - U.A.E.
Family 3 - U.A.E.
Family 4 - U.A.E.
Family 5 - Oman
Family 6 - Oman
Family 7 - Oman
Family 8 - Oman
Family 9 - KSA
Family 10 - KSA
Family 11 - U.A.E.
Family 12 - U.A.E.
Family 13 - U.A.E.
Family 14 - Lebanon
mut/mut
wt/mut
wt/wt
TOP
stillbirth
d. 9 years
d. 7 months
d. 2 weeks
d. 8 days
c.159_162del
c.8_36del
c.719_722del
c.663_666delinsG
primary fibroblasts
peripheral blood ONT-seq


B
F1-II:1
F4-II:2
F7-II:1
F9-II:1
F14-II:1
2 mo
12 mo
7 yrs
9 yrs
12 yrs
8 mo
3 yrs
F2-II:3
F7-II:3

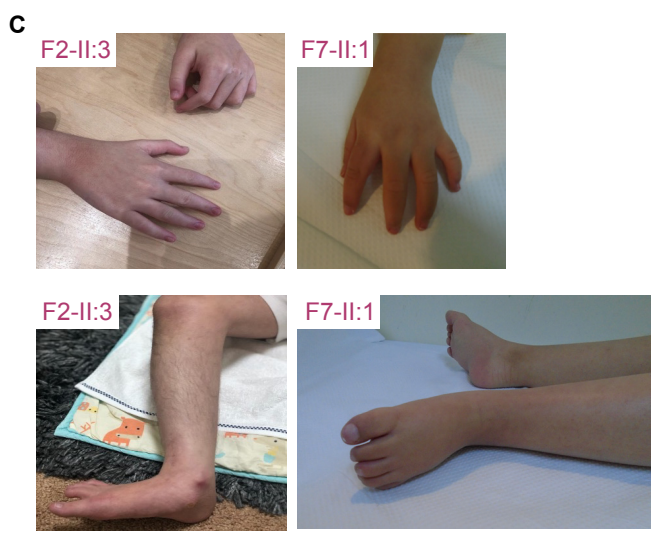
C
F2-II:3
F7-II:1
F2-II:3
F7-II:1

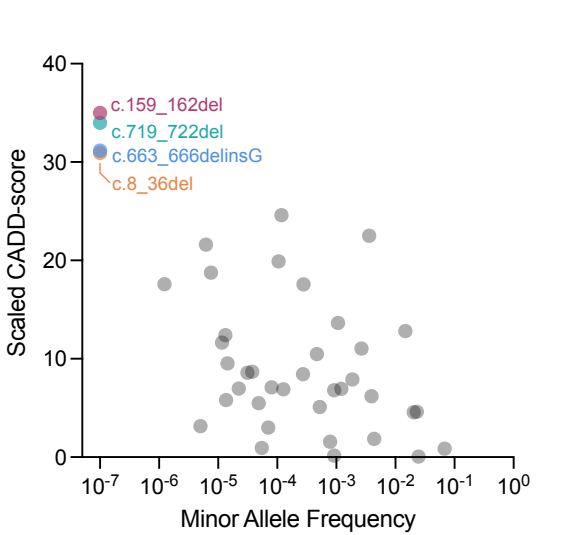
D
Scaled CADD-score
Minor Allele Frequency
c.159_162del
c.719_722del
c.663_666delinsG
c.8_36del

Figure 2

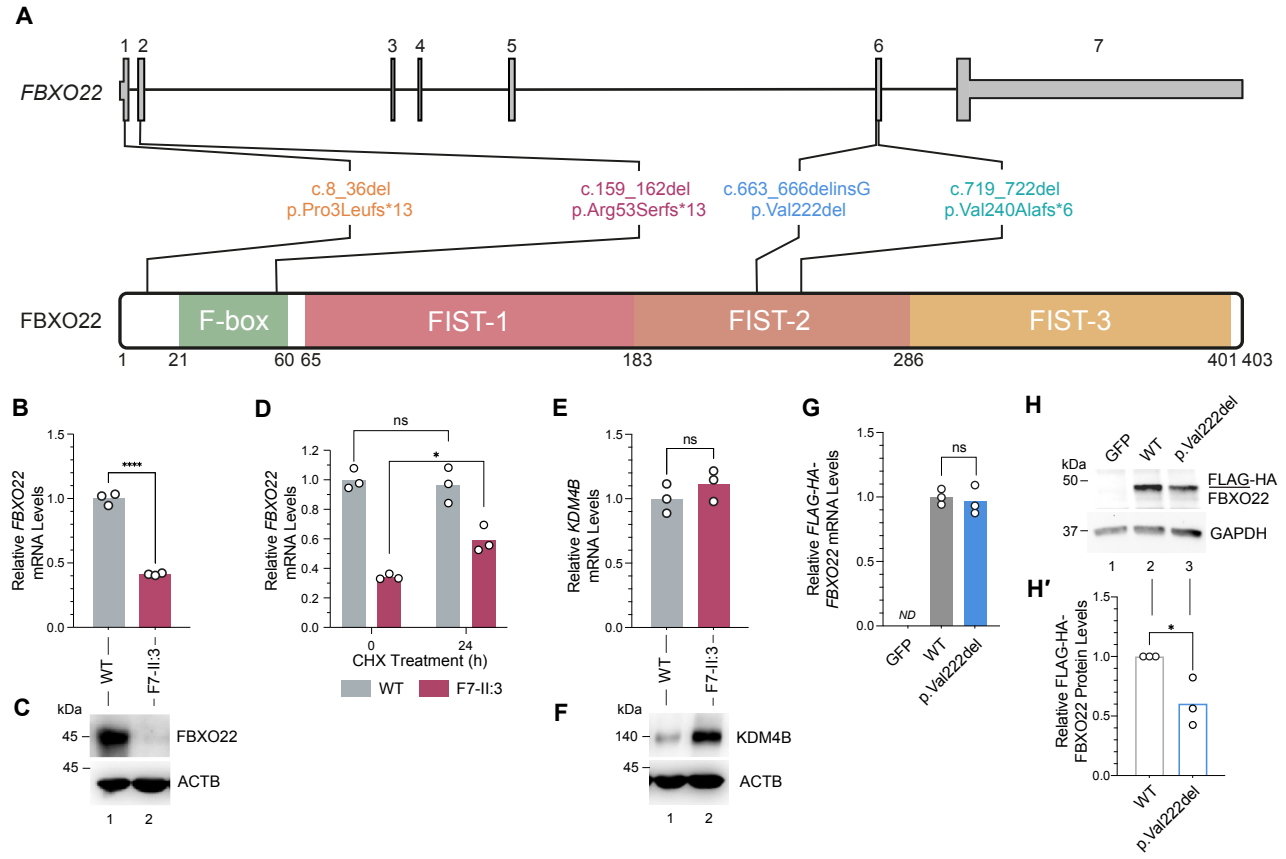
A
1 2 3 4 5 6 7
FBXO22
c.8_36del
p.Pro3Leufs*13
c.159_162del
p.Arg53Serfs*13
c.663_666delinsG
p.Val222del
c.719_722del
p.Val240Alafs*6
FBXO22
F-box
FIST-1
FIST-2
FIST-3
1 21 60 65 183 286 401 403
B
Relative FBXO22 mRNA Levels
****
WT
F7-II:3
C
kDa
45
FBXO22
45
ACTB
1 2
D
Relative FBXO22 mRNA Levels
ns
*
0 24
CHX Treatment (h)
WT
F7-II:3
E
Relative KDM4B mRNA Levels
ns
WT
F7-II:3
F
kDa
140
KDM4B
45
ACTB
1 2
G
Relative FLAG-HA-FBXO22 mRNA Levels
ns
ND
GFP
WT
p.Val222del
H
GFP
WT
p.Val222del
kDa
50
FLAG-HA
FBXO22
37
GAPDH
1 2 3
H'
Relative FLAG-HA-FBXO22 Protein Levels
*
WT
p.Val222del

Figure 3

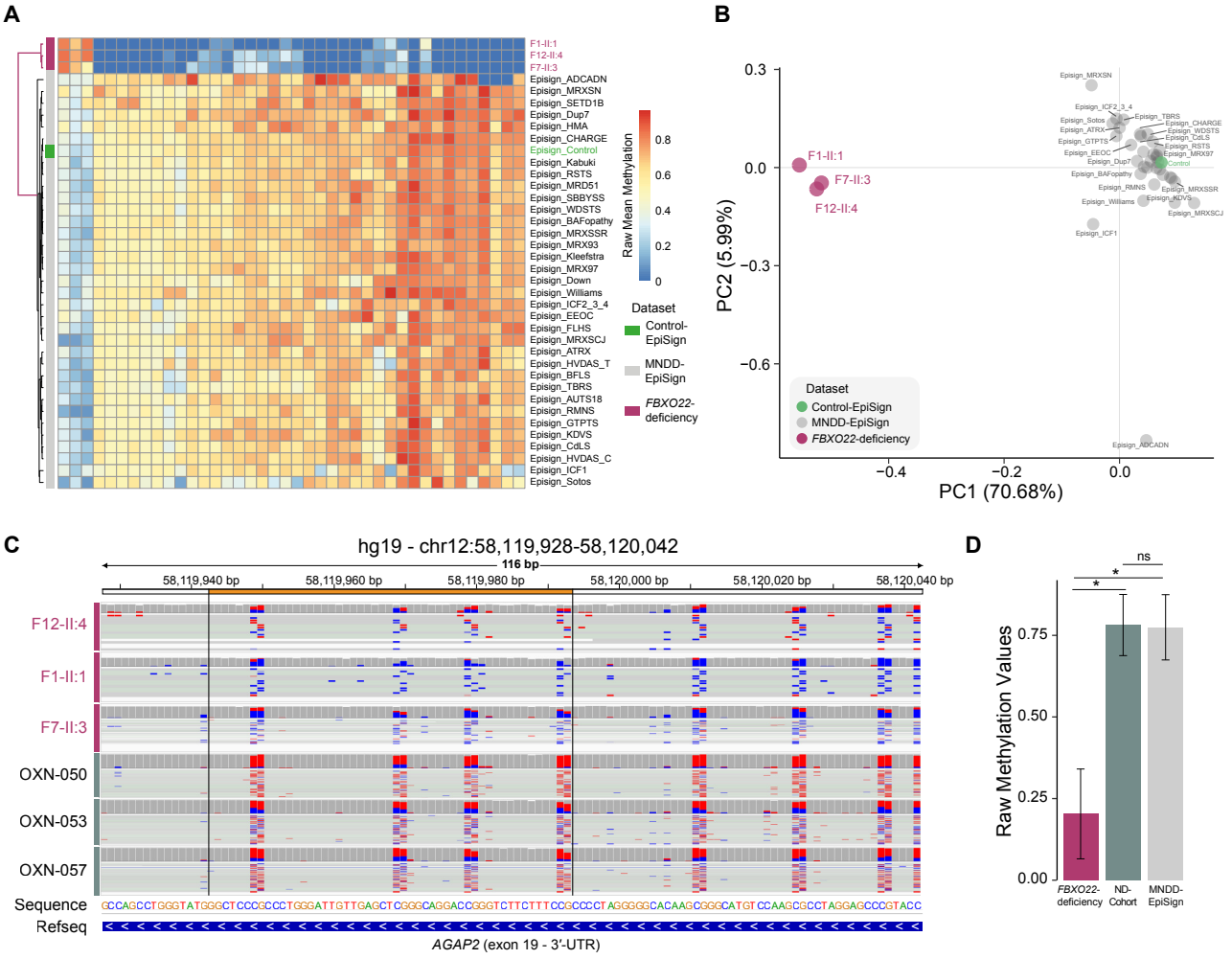
A
F1-II:1
F12-II:4
F7-II:3
Episign_ADCADN
Episign_MRXSN
Episign_SETD1B
Episign_Dup7
Episign_HMA
Episign_CHARGE
Episign_Control
Episign_Kabuki
Episign_RSTS
Episign_MRD51
Episign_SBBYSS
Episign_WDSTS
Episign_BAFopathy
Episign_MRXSSR
Episign_MRX93
Episign_Kleefstra
Episign_MRX97
Episign_Down
Episign_Williams
Episign_ICF2_3_4
Episign_EEOC
Episign_FLHS
Episign_MRXSCJ
Episign_ATRX
Episign_HVDAS_T
Episign_BFLS
Episign_TBRS
Episign_AUTS18
Episign_RMNS
Episign_GTPTS
Episign_KDVS
Episign_CdLS
Episign_HVDAS_C
Episign_ICF1
Episign_Sotos
Raw Mean Methylation
0.8
0.6
0.4
0.2
0
Dataset
Control-EpiSign
MNDD-EpiSign
FBXO22-deficiency
B
0.3
0.0
−0.3
−0.6
PC2 (5.99%)
F1-II:1
F7-II:3
F12-II:4
−0.4
−0.2
0.0
PC1 (70.68%)
Dataset
Control-EpiSign
MNDD-EpiSign
FBXO22-deficiency
C
hg19 - chr12:58,119,928-58,120,042
116 bp
58,119,940 bp
58,119,960 bp
58,119,980 bp
58,120,000 bp
58,120,020 bp
58,120,040 bp
F12-II:4
F1-II:1
F7-II:3
OXN-050
OXN-053
OXN-057
Sequence
Refseq
AGAP2 (exon 19 - 3′-UTR)
D
ns
*
*
Raw Methylation Values
0.75
0.50
0.25
0.00
FBXO22-deficiency
ND-Cohort
MNDD-EpiSign